

# Explainable Attention for Few-shot Learning and Beyond

Bahareh Nikpour<sup>1,2</sup>, Narges Armanfard<sup>1,2</sup>

<sup>1</sup>Department of Electrical and Computer Engineering, McGill University

<sup>2</sup>Mila - Quebec AI Institute, Montreal, QC, Canada  
{bahareh.nikpour, narges.armanfard}@mcgill.ca

## Abstract

Attention mechanisms have exhibited promising potential in enhancing learning models by identifying salient portions of input data. This is particularly valuable in scenarios where limited training samples are accessible due to challenges in data collection and labeling. Drawing inspiration from human recognition processes, we posit that an AI baseline’s performance could be more accurate and dependable if it is exposed to essential segments of raw data rather than the entire input dataset, akin to human perception. However, the task of selecting these informative data segments, referred to as hard attention finding, presents a formidable challenge. In situations with few training samples, existing studies struggle to locate such informative regions due to the large number of training parameters that cannot be effectively learned from the available limited samples. In this study, we introduce a novel and practical framework for achieving explainable hard attention finding, specifically tailored for few-shot learning scenarios, called FewXAT. Our approach employs deep reinforcement learning to implement the concept of hard attention, directly impacting raw input data and thus rendering the process interpretable for human understanding. Through extensive experimentation across various benchmark datasets, we demonstrate the efficacy of our proposed method.

## Introduction

Deep learning algorithms have demonstrated effectiveness in modeling and representing data when a substantial quantity of labeled data is accessible. However, they struggle to adapt to scenarios where only a few examples per class are available for training. That is while it is often expensive and labor-intensive to prepare labeled data. Additionally, the subjective nature of data labeling and its dependence on individual annotators presents additional complexities. To deal with these challenges, few-shot learning is introduced to the field of machine learning, where the goal is training a model with limited labeled data and generalize its knowledge to new, unseen classes (Shi et al. 2021). There are lots of practical applications for few-shot learning methods ranging from computer vision such as image classification (Dhillon et al. 2019), activity recognition (Kumar Dwivedi et al. 2019), image retrieval (Wang, Gui, and Hebert 2017), and

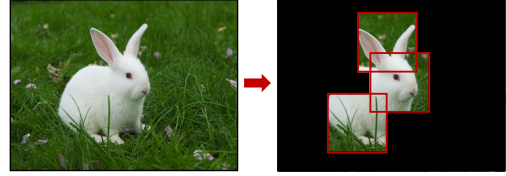


Figure 1: The three attentive regions to define the class rabbit

object tracking (Majee, Agrawal, and Subramanian 2021) to robotics and medical applications such as drug discovery (Vella and Ebejer 2022). Most of the leading few-shot learning methods are either metric learning-based or meta learner-based (Li et al. 2017). Prototypical Networks (Prot-Net) is one of the most popular metric-based approaches in few-shot learning, proposed by Snell et al. (Snell, Swersky, and Zemel 2017). The main idea behind Prototypical Networks is to learn a metric space where examples from the same class are close to each other and examples from different classes are far apart.

In recent years, attention mechanisms have emerged as a powerful tool for improving computer vision algorithms by enabling models to focus on discriminative regions within the image (Liu, Johns, and Davison 2019). That is because not all sections of images possess equal importance, and only certain regions hold valuable information. Attention is particularly inspired by the human visual system which has the ability to focus on specific parts of a scene to rapidly comprehend it. The attention models in the literature mainly fall under two categories: “soft attention”, where different weights show the importance of different data parts, and “hard attention”, where only the important parts of the data are kept and the rest are discarded, allowing for a more interpretable process. Hard attention was first put in place by Minh et al. (Mnih et al. 2014) to reduce computation in convolutional neural networks. Later on, many other techniques were introduced to find hard attention such as (Ranzato 2014; Alexe et al. 2012; Ba et al. 2015; Seifi, Jha, and Tuytelaars 2021; Rangrej and Clark 2021). One important benefit of hard attention over soft attention is improving computational efficiency by reducing the data size.

Finding hard attention is advantageous in few-shot learning as there are few samples per class and the learning

method can be easily misled by noise, background clutter, and uninformative regions. However, previous studies have encountered difficulties in identifying these informative regions because of the large number of parameters that cannot be learned from the available limited samples.

In this paper, we propose a novel explainable hard attention-finding approach for few-shot learning, called FewXAT, to detect the attentive areas and enhance performance in few-shot learning. Our method finds hard attention, i.e. informative regions, within an image during the few-shot learning process utilizing deep reinforcement learning. By focusing on the attentive regions, the model can effectively capture the essential cues necessary for accurate classification, even with limited training samples. The proposed FewXAT framework formulates the problem of finding and detecting attentive regions as a Markov Decision Process (MDP), where a reinforcement learning agent is responsible for finding the optimum locations of multiple attentive areas, called patches, within an image. The agent receives feedback in the form of rewards from the few-shot baseline classifier, guiding it to identify patches that contribute most to the final classification decision. Through this iterative process, the agent becomes adept at identifying informative patches, which facilitates generalization and robustness in scenarios with limited labeled data. In addition, keeping only the informative patches and discarding the rest of the information would decrease the memory and computational complexity of the learning model. To enhance the training process, we add an auxiliary task, which is a contrastive learning module, to help finding a better representation of the data.

Deep Reinforcement Learning (RL), has been very successful in several computer vision tasks (Mnih et al. 2013; Wang et al. 2018; Yun et al. 2017; Nikpour and Armanfard 2023a, 2021; Nikpour, Sinodinos, and Armanfard 2022; Nikpour and Armanfard 2023b). It has also been used in several research to find hard attention in RGB images for classification tasks such as (Ba, Mnih, and Kavukcuoglu 2014; Elsayed, Kornblith, and Le 2019). Moreover, there are a few methods in the literature aiming at finding soft attention in few-shot learning (Yan et al. 2019; Ren et al. 2019; Hong et al. 2021). There is one research exploring the idea of finding soft attention in the context of few-shot learning, where the attention is found on the feature map extracted by convolution layers (Hong et al. 2021). Different from this method, we aim to find hard attention in the original image. To the best of our knowledge, FewXAT is the first work exploring the idea of finding hard attention for the RGB images in the context of few-shot learning. Moreover, the existing hard attention-finding methods in the classification task have very complex structures, making them impossible to train for few-shot learning setup.

The contributions of our method are listed below:

- We discovered the novel problem of hard attention finding for RGB images in a few-shot learning setup.
- We proposed a simple framework to address this problem using deep reinforcement learning.
- We added a contrastive learning module, as an auxiliary task, to enhance the training process.

- We conducted experiments on four popular benchmark datasets and got competitive results, despite using a small portion of the data, showing the effectiveness of FewXAT.
- By finding hard attention, i.e. attentive regions in the images, we enhance the contextual understanding and interpretability of the baseline’s predictions.
- By attending to only the informative parts of the image and discarding the rest, our method can decrease the size of the data noticeably which leads to a decrease in the baseline model’s complexity.
- We explored the performance of our proposed method in the classification task, proving the usefulness of our method in other tasks as well.

## Methodology

In the following we first begin by introducing the terminology employed in few-shot learning, then we present our proposed method in detail.

### Problem setting

In few-shot learning, an **episode**<sup>1</sup> refers to a single learning task where a model has to learn from a limited amount of data. The few-shot model learns during many **episode**. Typically, an **episode** consists of two main components: a Support set and a Query set. To train a model, a support set and a query set are randomly selected from the data in each **episode**. This approach to learning is commonly referred to as “ $N$ -way,  $G$ -shot” classification, where there are  $N$  classes and  $G$  samples for each class in the support and query sets. We denote the support set as  $SU = \{(x_j, y_j)\}_{j=1}^{N \times G}$ , where  $x_j$  is the  $j^{th}$  sample in the support set and  $y_j$  is its corresponding label.

### Proposed method

We assume that every object can be recognized by a maximum of three important regions. Such important regions for recognizing a rabbit are shown in Figure 1. As such, FewXAT aims to detect three attentive image patches that can also overlap. The size of each patch is fixed and set to  $\lfloor 1/3 \rfloor$  of the overall size of the input image. So, FewXAT keeps maximum  $1/3$  of an image.

The block diagram of the proposed method is shown in Figure 2. FewXAT consists of three main modules: an RL module, which is responsible for finding the attentive regions, the baseline classifier module, for learning the final classification task, and a contrastive learning module which we add as an auxiliary task to improve the performance and generalization of the model. In summary, in the RL module, the state is defined using the data and is fed to the agent. The agent completes an episode of  $K$  steps and gets a reward and calculates the loss of the RL module, i.e.  $L_{RL}$ . The

<sup>1</sup>Two types of episodes are used in this paper: the **episode** in the few-shot setup and the episode in the reinforcement learning framework. To avoid confusion, we use the bold-sized word to define the few-shot **episode**.

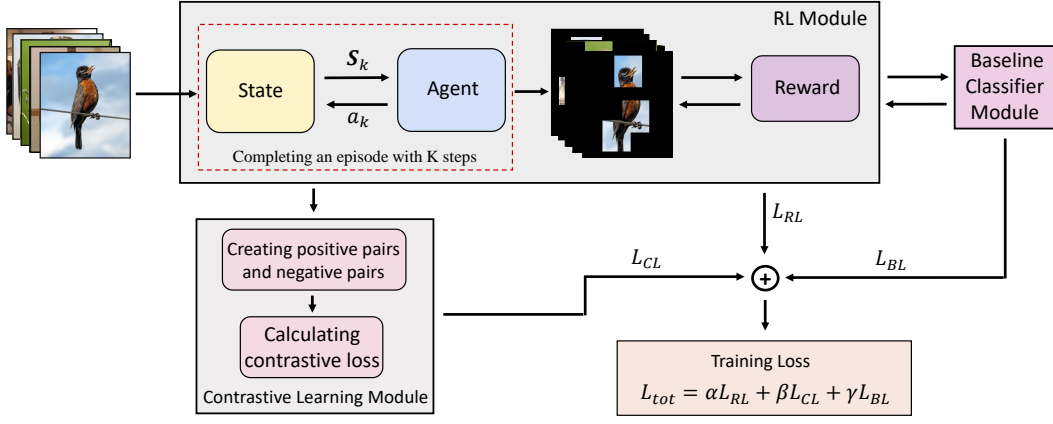


Figure 2: Block diagram of the proposed FewXAT method.

reward is generated by applying the baseline classifier to the attentive regions of the validation set. The agent output on the input training data, which includes the three selected patches per image, are given to the baseline classifier to calculate the classifier loss, i.e.,  $L_{BL}$ . Moreover, the agent output on the training data is used to create positive and negative pairs to be used to calculate the contrastive loss, i.e.  $L_{CL}$ . At the end, these three losses are added with different weights to generate the total loss,  $L_{tot}$ , that is used to update the networks of all the three modules. The details regarding each module are discussed in the following.

### 1- RL Module

In our method, we model the process of finding the attentive areas in images as a Markov decision process and solve it with the popular policy-based reinforcement learning algorithm, Monte Carlo policy gradient (REINFORCE) (Williams 1992). The agent in its current state takes actions that result in changing its state and receiving a reward. The agent learns to select the important areas in the image, i.e., it finds spatial hard attentions, by maximizing the total expected reward. In this paper the RL agent is run for every images in a batch with size  $M$ , and the  $k^{th}$  step in the RL episode for the  $m^{th}$  sample in the batch is denoted by  $\mathcal{T}_{k,m} = (S_{k,m}, A_{k,m}, R_k)$ , where  $S_{k,m}$ ,  $A_{k,m}$ , and  $R_k$  are state, action, and reward at the  $k^{th}$  step for the  $m^{th}$  image in the batch. One single episode is denoted as  $\mathcal{T}_m = (S_{1,m}, A_{1,m}, R_1, \dots, S_{K,m}, A_{K,m}, R_K)$ . State, agent, action, and reward in the proposed process are as follows:

**State:** We define the state  $S_{k,m}, m = 1, \dots, M$  as the concatenation of the  $m^{th}$  original image in the batch,  $I_m$ , and the output of the agent with the selected areas in the previous step of the episode,  $I_{k,m}$ , i.e.  $S_{k,m} = [I_m, I_{k,m}]$ .  $I_{k,m}$  has the same size as the original  $I_m$ , where only the selected patches are present in the image and all the remaining parts are set to zero.  $I_{k,m}$  is shown in the right side of Figure 3. In the initial state  $S_{0,m}$ ,  $I_{0,m}$  is initiated such that the patches are located side-by-side at the top of the image as can be seen in Figure 4.

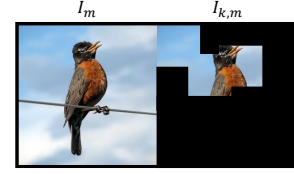


Figure 3: The agent's state  $S_{k,m}$ , which is concatenation of the original image  $I_m$ , and the image output of the agent in the  $k^{th}$  step of the episode  $I_{k,m}$ , i.e.  $S_{k,m} = [I_m, I_{k,m}]$

**Agent:** The agent can be any neural network structure that is capable of dealing with image data. At each step of the episode, i.e. the  $k^{th}$  step, and for the  $m^{th}$  image, the agent outputs the probability matrix  $P_{k,m}$  which will be used to define the actions it should take.

**Action:** The action defines the direction of movements of the patches. Therefore, for each patch, five actions have been designed: go up, down, left, right, and apply no change. The movement step size is set to  $b$ . In our experiments,  $b$  is set to 3 pixels for all datasets. For the  $m^{th}$  image, each action is denoted by  $a_{k,m}^l$  where  $k$  refers to the  $k^{th}$  step of the RL episode and  $l \in \{1, 2, 3\}$  shows the  $l^{th}$  attentive region. The actions are sampled from a Bernoulli distribution over the

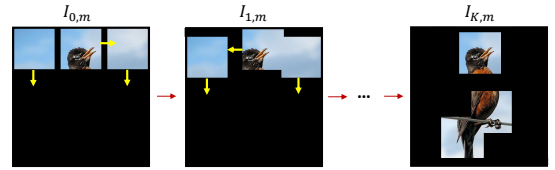


Figure 4: An example of  $I_{k,m}, \{k = 0, \dots, K\}$  during one episode in our proposed method. The actions, shown in yellow arrows, for step 1 are go down ( $\downarrow$ ), go right ( $\rightarrow$ ), and go down ( $\downarrow$ ) for the first, second, and third regions respectively, which results in  $I_{1,m}$ . After completing an episode, the agent outputs the regions found in  $I_{K,m}$ .

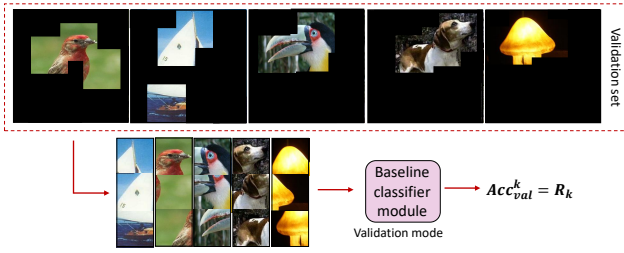


Figure 5: An example of validation batch after finding the attentive region in in step  $k$ . To get the reward, the new batch of validation samples are given to the baseline and the output accuracy is considered as the reward.

probability output of agent,  $P_{k,m} = \{p_{k,m}^l\}_{l=1}^3$  as below:

$$A_{k,m} = \{a_{k,m}^l \sim \text{Bernoulli}(p_{k,m}^l)\}_{l=1}^3 \quad (1)$$

An example of one episode is depicted in Figure 4.

**Reward:** The reward should reflect how good the action of the agent is in reaching its goal. In our method, the goal is improving or maintaining the baseline’s performance while reducing the complexity (and hence improving interpretability). Therefore, the baseline is used to evaluate the output of the agent in step  $k$  of the episode. We evaluate the agent’s performance at the  $k^{\text{th}}$  step, by applying it to a random batch of a validation set with  $N \times G$  samples for both support and query sets. Using a validation set increases the method’s generalization ability. To obtain the reward, first, we let the agent find the three attentive regions in each image of the validation set; then, the three regions are concatenated next to each other, as is shown in Figure 5. Then, it is fed to the baseline in the validation mode to get accuracy. The validation accuracy i.e.  $Acc_{val}^k$  is considered as the reward as is defined below:

$$R_k = Acc_{val}^k \quad (2)$$

**Training with REINFORCE:** The goal of our reinforcement learning agent is learning a policy function (which finds optimum locations of attentive areas) by maximizing the expected reward  $\mathcal{R}(\theta)$  shown below:

$$\mathcal{R}(\theta) = \mathbb{E}_{p_{\theta}(a_{k,m}^l)}[R_k], \quad (3)$$

where  $p_{\theta}(a_{k,m}^l)$  is the probability distribution of the possible actions for the  $l^{\text{th}}$  patch, and  $\mathbb{E}$  shows the expectation over  $l$ ,  $m$  and  $k$  where  $l = \{1, \dots, 3\}$ ,  $k = \{1, \dots, K\}$  and  $m = \{1, \dots, M\}$ . We utilize REINFORCE, which is a popular policy gradient algorithm(Williams 1992) to maximize the expected reward and therefore find the optimal parameter  $\theta$  for the policy. The policy is approximated by a function that is parameterized by  $\theta$ . Following REINFORCE, the gradient of the expected reward in the  $k^{\text{th}}$  step of the episode, with respect to the parameter  $\theta$  is found as below:

$$\nabla_{\theta} \mathcal{R}(\theta) = \mathbb{E}_{p_{\theta}(a_{k,m}^l)}[R_k \nabla_{\theta} \ln \pi_{\theta}(a_{k,m}^l | S_{k,m})], \quad (4)$$

where  $\pi_{\theta}$  denotes the policy function, and  $S_{k,m}$  is the state of the  $m^{\text{th}}$  image in the batch at the  $k^{\text{th}}$  step as  $S_{k,m} = [I_m, I_{k,m}]$ . As was mentioned before, during each episode, the agent takes  $K$  steps for each image in the batch. Therefore, we compute the average gradient over  $M$  samples in the batch as:

$$\nabla_{\theta} \mathcal{R}(\theta) \approx \frac{1}{KM} \sum_{k=1}^K [R_k \sum_{m=1}^M \sum_{l=1}^3 \nabla_{\theta} \ln \pi_{\theta}(a_{k,m}^l | S_{k,m})], \quad (5)$$

where  $a_{k,m}^l$  is the action for the  $l^{\text{th}}$  patch of the  $m^{\text{th}}$  image in the batch in the  $k^{\text{th}}$  step of the episode, and  $S_{k,m}$  is state of the  $m^{\text{th}}$  image in the batch.

In order to enhance convergence and decrease variance during the training of  $\theta$ , we normalize the reward by subtracting a constant baseline value  $c$ . This baseline  $c$  corresponds to the mean reward across episode. Hence, the gradient becomes:

$$\nabla_{\theta} \mathcal{R}(\theta) \approx \frac{1}{KM} \sum_{k=1}^K [(R_k - c) \sum_{m=1}^M \sum_{l=1}^3 \nabla_{\theta} \ln \pi_{\theta}(a_{k,m}^l | S_{k,m})], \quad (6)$$

Therefore, the loss of policy to minimize can be shown as:

$$L_{RL} = \frac{1}{KM} \sum_{k=1}^K [(R_k - c) \sum_{m=1}^M \sum_{l=1}^3 \ln \pi_{\theta}(a_{k,m}^l | S_{k,m})] \quad (7)$$

**2- Training the Baseline model:** The baseline is responsible for learning the desired task, which is classification of few-shot samples using only the selected patches. We train the baseline during policy training using the train data. To do so, the output attentive regions, provided by the policy network, corresponding to the training data are concatenated next to each other (similar to what was done for the validation set when obtaining the reward, shown in Figure 5). More specifically, the concatenation of three selected patches from each training image generates a new image that is three times the size of a single patch. The new images are used as training data for the baseline model. The baseline loss  $L_{BL}$ , defined in (??), is calculated on its training data. Note that any few-shot classification method can be used as the FewXAT baseline module. In this paper, we used the ProtoNet algorithm as the baseline, as it is one of the most popular and well-performing learning methods for few-shot learning (Snell, Swersky, and Zemel 2017). For each class, ProtoNet calculates a prototype vector by averaging the embeddings (obtained from a neural network) of the support samples belonging to that class in the feature space. The prototype represents the characteristic features of the class. During training, ProtoNet minimizes the distance between the embedding of a query sample and the prototype of the query sample’s true class, while maximizing the distance from the prototypes of other classes. This encourages the model to learn prototypes that can effectively represent classes and differentiate them. The loss of ProtoNet is calculated as:

$$L_{BL} = -\log(\text{softmax}(-||g(x_q), v_y||)) \quad (8)$$

where  $g(x_q)$  is the embedded representation of the query sample,  $v_y$  is the prototype representation of the correct class  $y$  in the support set  $SU$ ,  $\|\cdot\|$  denotes the distance (e.g., Euclidean) between two vectors, and  $\text{softmax}(\cdot)$  computes the softmax function over the negative distance.

**3- Contrastive Learning Module:** In general, adding auxiliary tasks is advantageous from various perspectives. It can improve the performance of the main task and help to increase the generalization by encouraging the model to learn more general features. Moreover, learning the auxiliary task along with the main task usually helps with faster convergence, by providing additional gradients that guide the learning process and can prevent the model from getting stuck in local minima. Lastly, the auxiliary task can force the model to learn meaningful and disentangled representations of the input data, making it easier to extract important features and patterns. Motivated by the mentioned benefits, we added the contrastive learning module as an auxiliary task to help the training procedure of our method.

Contrastive learning is a learning technique that aims to learn useful representations by bringing similar data samples, i.e. positives, closer to each other in the learned representation space while pushing dissimilar data points, i.e. negatives, farther apart. In our method, we use the support set and query set in the batch to create positive and negative pairs. Pairs from the same class and their augmentation are considered as positive pairs, while negative pairs are pairs from different classes. The augmentations we used for each sample are: (1) every possible permutation of concatenating the three selected attentive regions next to each other, as we do not want our method to be sensitive to the concatenation order of the selected patches; (2) a random rotation in the range -45 degrees and 45 degrees, to make our method robust to rotation. Therefore, we have 12 augmentations, and 12 positive pairs as a result, for each sample as can be seen in Figure 6. After augmentation and creating positive and negative pairs, the contrastive loss is calculated. As the labels of data samples are available, we use the supervised contrastive loss (SupCon loss) (Khosla et al. 2020) as follows:

$$L_{CL} = \sum_{i \in W} \frac{-1}{|O(i)|} \sum_{o \in O(i)} \log \frac{\exp(f_i \cdot f_o / \tau)}{\sum_{u \in U(i)} \exp(f_i \cdot f_u / \tau)} \quad (9)$$

where  $i \in W \equiv \{1, \dots, 2Z\}$ , is the index of an arbitrary augmented sample ( $Z$  is the number of randomly sampled pairs).  $O(i)$  shows the indices of the positive pairs distinct from  $i$ , and  $|O(i)|$  denotes its cardinality,  $U(i) \equiv W \setminus i$ ,  $f_\zeta$  shows the output representation of the network for the  $\zeta$ th index, and  $\tau$  is the temperature parameter to control the similarity scale. For more details, see (Khosla et al. 2020).

#### 4- Training the algorithm

After calculation of the three losses, i.e. the policy loss, the baseline loss and the contrastive learning loss, the total loss to be minimized is calculated as:

$$L_{tot} = \alpha L_{RL} + \beta L_{CL} + \gamma L_{BL} \quad (10)$$

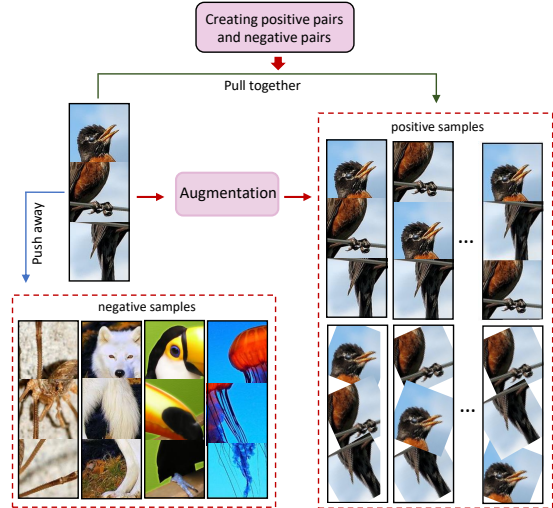


Figure 6: An example of creating positive and negative pairs in 5-way scenario. The first row in positive samples shows every permutation of the attentive regions. The second row shows the rotated attentive regions and their permutation.

where  $\alpha$ ,  $\beta$ , and  $\gamma$  are hyperparameters to control the contribution of their corresponding loss term. The pseudo-code of the proposed FewXAT framework is presented in Algorithm 1. In summary, a batch of few-shot tasks is firstly sampled and the training data, including both support set and query set, is given to the agent,  $K$  steps are completed, and the reward  $R_k$  is calculated in each step  $k$  of the method. The output of the agent is the coordinated of the three patches. Using the output of the agent, the new train set including samples with the attentive regions is created and the loss of baseline is found using this new set. Then, the CL loss is computed using the output embedding of the contrastive learning network on the data and its augmentation. Having the three losses, the total loss is calculated, and all the three networks are updated. This process is repeated for a defined number of **episodes** until the three networks are trained.

In the testing phase, the train data is first given to the policy, the selected patches are concatenated, and the baseline is trained on this new train set. Then, the test data is fed to the policy and the new test data obtained by concatenation of the selected patches is classified using the trained baseline.

## Experiments

To evaluate the effectiveness of our proposed FewXAT approach, we conducted experiments on four commonly employed datasets for few-shot learning, MiniImageNet (Ravi and Larochelle 2016), CIFAR-FS (Krizhevsky, Hinton et al. 2009), FC-100(Krizhevsky, Hinton et al. 2009), and CUB (Welinder et al. 2010), and as was mentioned in the previous section, we selected ProtoNet (Snell, Swersky, and Zemel 2017) as the baseline. In the following, the details of every experiment are explained.

Table 1: The accuracy results (in percent) on MiniImageNet, CIFAR-FS, FC-100, and CUB datasets before and after applying FewXAT, and with random selection for 5-shot 5-way (5-s 5-w), and 1-shot 5-way (1-s 5-w) settings.

methods \ Dataset	MiniImageNet		CIFAR-FS		FC-100		CUB	
	5-s 5-w	1-s 5-w	5-s 5-w	1-s 5-w	5-s 5-w	1-s 5-w	5-s 5-w	1-s 5-w
<b>Conv-4</b>	66.98	48.12	77.98	67.12	48.74	31.47	75.12	50.46
<b>ResNet-10</b>	71.12	49.98	81.26	70.15	51.72	36.41	83.47	72.12
<b>Random(Conv-4)</b>	48.76	32.11	65.14	49.67	42.12	25.69	68.21	35.12
<b>Random(ResNet-10)</b>	53.76	36.12	70.06	55.14	45.22	29.88	70.32	37.03
<b>FewXAT(Conv-4)</b>	<b>68.32</b>	<b>48.89</b>	<b>78.23</b>	<b>67.94</b>	<b>50.21</b>	<b>31.87</b>	<b>76.11</b>	<b>53.21</b>
<b>FewXAT(ResNet-10)</b>	<b>73.96</b>	<b>52.72</b>	<b>82.47</b>	<b>69.94</b>	<b>53.28</b>	<b>37.91</b>	<b>83.12</b>	<b>73.79</b>

Table 2: The accuracy results of FewXAT with and without including the Contrastive Learning module on MiniImageNet, CIFAR-FS, FC-100, and CUB datasets with ProtoNet(ResNet-10) as baseline, for 5-shot 5-way (5-s 5-w), and 1-shot 5-way (1-s 5-w) settings.

methods \ Dataset	MiniImageNet		CIFAR-FS		FC-100		CUB	
	5-s 5-w	1-s 5-w	5-s 5-w	1-s 5-w	5-s 5-w	1-s 5-w	5-s 5-w	1-s 5-w
<b>FewXAT with the CL module</b>	<b>73.96</b>	<b>52.72</b>	<b>82.47</b>	<b>69.94</b>	<b>53.28</b>	<b>37.91</b>	<b>83.12</b>	<b>73.79</b>
<b>FewXAT without the CL module</b>	65.22	49.18	79.34	66.82	49.47	35.22	78.34	69.57

Algorithm 1: The proposed FewXAT method

**Input:** The training and validation images and their labels

**Output:** Trained Agent

- 1: Initialize the Agent, the baseline, and the Contrastive Learning network.
- 2: **for** episodes **do**
- 3:   Sample a batch of tasks
- 4:   **for**  $K$  steps **do**
- 5:     The agent takes a step.
- 6:     Find the reward  $R_k$  by eq. 2.
- 7:   **end for**
- 8:   Find the agent’s loss ( $L_{RL}$ ) using eq. 7.
- 9:   Create the new train set and find the baseline’s loss ( $L_{BL}$ ).
- 10:   Create data augmentation and find the SupCon loss ( $L_{CL}$ ) using eq. 9.
- 11:   Find the total loss  $L_{tot}$  using eq. 10
- 12:   Update the three networks.
- 13: **end for**
- 14: **return** The trained Agent

### FewXAT for fewshot

To evaluate FewXAT, we used ProtoNet with two different structures including Conv-4, and ResNet-10. The accuracy results are shown in Table 1, for the datasets MiniImageNet, CIFAR-FS, FC-100, and CUB. The first row of the table shows the test results of the baselines on the original data. The second row presents the testing results of baselines after randomly picking three patches in images from a uniform distribution. The last row gives the accuracy results after finding the attentive areas by our proposed FewXAT method. In the cases where the accuracy after applying FewXAT,

FewXAT(baseline), is in the range [baseline accuracy - 0.5, baseline accuracy + 0.5], i.e. the difference of the accuracy before and after applying FewXAT is less than 0.5, we assume the performance is maintained and in the cases where the accuracy of FewXAT(baseline) > baseline accuracy + 0.5, we assume we have improvement. As can be seen, the accuracy is either improved or maintained in all the cases after keeping the attentive regions and discarding the rest of the data. This is specifically beneficial as, firstly, by downsizing the images, the complexity is decreased, and secondly, by keeping the important regions, the interpretability is improved. In addition, comparing the results of FewXAT with the random selection, all the results are remarkably better, indicating the proposed method learns to find the optimum locations that result in improved performance.

### Visualization of the learned hard attention

The output of our proposed FewXAT method, i.e. the detected regions for some images from miniImageNet data is visualized in Figure 7. For example, in the first image which belongs to the class dog, the eyes and nose of the dog are detected as the attentive regions that can discriminate it from other classes. Also, less than one-third of the image is kept, which decreases the data size significantly. The visualized output of FewXAT confirms that its output is consistent with human perception and makes the learning model interpretable.

### Effect of Contrastive Learning module

To see how adding this auxiliary task, i.e. contrastive learning (CL), affects the performance, we removed this module from our method and ran it for our datasets using ProtoNet (with ResNet-10). The accuracy results are reported in Table 2. As can be seen, adding the CL module can significantly

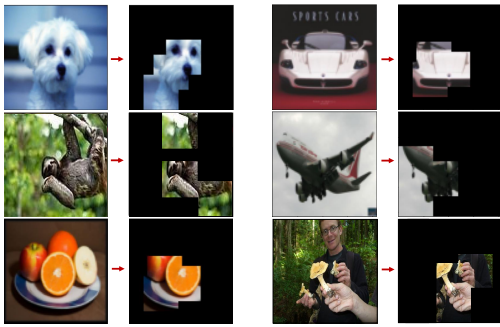


Figure 7: Visualization of the attentive regions found by FewXAT

improve the performance by leading the model to learn better representations. It is specifically important in a few-shot setting, where there exist few samples leading to poor generalization ability of the classification model. Adding the CL module helps in learning semantically meaningful features, resulting in enhanced generalization.

### Influence of hyperparameters $b$ and $K$

As was discussed,  $b$  denotes the step size of the agent to go right/left/up/down, and  $K$  is the total number of steps that the agent completes during an episode. The choice of these hyperparameters are highly correlated, and both should be selected in such a way that gives the agent the capability of spanning all the image. To see their effect on the performance of our method, we picked these parameters from the set:  $\{(b, K) : (1, 20), (1, 40), (3, 20), (7, 15)\}$  and the results of applying FewXAT on miniImagenet using Protonet(Conv-4) are reported in Table 3. The size of images are  $84 \times 84$ . As can be seen, by setting the step size to 1, which is very small, completing 20 steps is not enough to explore all the images, and by doubling the step size, the performance has improved significantly. However, increasing  $K$  slows down the training process, which is not desired. Setting  $b$  to 7, which is a large step size, does not yield an acceptable result as it causes the agent to jump from some important and informative regions and never find them. Therefore, there should be a trade-off in selecting  $b$  and  $K$ . The slower step size has a positive effect on the performance, but makes the policy training too slow. On the other hand, setting it too large can disrupt the search process. We picked  $(3, 20)$ , as the best values for our method.

### Run time improvement

The Proposed FewXAT method reduces the data size by keeping the maximum of  $1/3$  of the image; therefore, the

Table 3: Accuracy results using different  $b, K$  values.

(b, K)	(1,20)	(1,40)	(3,20)	(7,15)
5-s 5-w	56.98	68.43	68.32	53.21

Table 4: Run time (in hours) of training ProtoNet (with Conv-4) with and without FewXAT.

MiniImageNet	5-s 5-w		1-s 5-w	
	training	testing	training	testing
With FewXAT	10.23	0.15	4.16	0.03
Without FewXAT	21.33	0.22	12.32	0.12

number of parameters needed to train the baseline classifier reduces, leading to faster training and testing of it. To prove this argument, we train and test our baseline, which is ProtoNet (with Conv-4), on miniImageNet with the original data, and with only the three selected attentive regions and compare their run time which are presented in Table 4. The first row shows the training and testing run time of the baseline after selecting the attentive regions in the images while the second row shows these run times with the original data. As was expected, by selecting the attentive areas, the run time significantly decreases in both the training and testing phases, which is especially beneficial for resource efficiency and online applications. One Tesla P100-PCIE-16GB GPU is used to run these experiments.

### Beyond few-shot learning

To show the effectiveness of our proposed method on other tasks rather than few-shot learning, we chose the classification task of two popular benchmark datasets which are ImageNet10 and ImageNetdog. The two datasets are subsets of the popular ImageNet data. As the baseline, we selected Conv-4, and ResNet-50. The accuracy results before and after applying FewXAT, i.e. selecting the attentive are presented in Table 5. The last row of the table indicates our proposed method could improve the performance of the baseline models while removing the redundant information and reducing the data size as a result. This experiment confirms the proposed framework is not only advantageous in few-shot learning, but it can go beyond that and be used in other tasks such as classification and representation learning while providing an interpretable patch selection.

### Conclusion

Our paper introduces FewXAT, a novel Explainable Attention mechanism designed to enhance few-shot learning performance by finding hard attention. We used deep reinforcement learning to detect attentive regions. Our hypothesis was

Table 5: Classification accuracy (in percent) of the two different baseline models with and without FewXAT.

Method	ImageNet10	ImageDog
Conv-4	66.08	53.21
ResNet50	70.23	58.94
FewXAT(Conv-4)	69.27	56.11
FewXAT(ResNet50)	72.18	60.64

that by identifying informative patches within images, we could improve the adaptability of models to new classes with limited labeled data. Experimental results support the efficacy of our approach, showing performance improvements or maintenance in few-shot learning tasks along with a significant decrease in complexity and enhanced interpretability. The FewXAT method demonstrates promising results in the classification task as well, indicating its potential applicability in broader computer vision tasks.

## References

- Alexe, B.; Heess, N.; Teh, Y.; and Ferrari, V. 2012. Searching for objects driven by context. *Advances in Neural Information Processing Systems*, 25.
- Ba, J.; Mnih, V.; and Kavukcuoglu, K. 2014. Multiple object recognition with visual attention. *arXiv preprint arXiv:1412.7755*.
- Ba, J.; Salakhutdinov, R. R.; Grosse, R. B.; and Frey, B. J. 2015. Learning wake-sleep recurrent attention models. *Advances in Neural Information Processing Systems*, 28.
- Dhillon, G. S.; Chaudhari, P.; Ravichandran, A.; and Soatto, S. 2019. A baseline for few-shot image classification. *arXiv preprint arXiv:1909.02729*.
- Elsayed, G.; Kornblith, S.; and Le, Q. V. 2019. Saccader: Improving accuracy of hard attention models for vision. *Advances in Neural Information Processing Systems*, 32.
- Hong, J.; Fang, P.; Li, W.; Zhang, T.; Simon, C.; Harandi, M.; and Petersson, L. 2021. Reinforced attention for few-shot learning and beyond. In *Proceedings of the IEEE/CVF Conference on Computer Vision and Pattern Recognition*, 913–923.
- Khosla, P.; Teterwak, P.; Wang, C.; Sarna, A.; Tian, Y.; Isola, P.; Maschinot, A.; Liu, C.; and Krishnan, D. 2020. Supervised contrastive learning. *Advances in neural information processing systems*, 33: 18661–18673.
- Krizhevsky, A.; Hinton, G.; et al. 2009. Learning multiple layers of features from tiny images.
- Kumar Dwivedi, S.; Gupta, V.; Mitra, R.; Ahmed, S.; and Jain, A. 2019. Protogan: Towards few shot learning for action recognition. In *Proceedings of the IEEE/CVF International Conference on Computer Vision Workshops*, 0–0.
- Li, Z.; Zhou, F.; Chen, F.; and Li, H. 2017. Meta-sgd: Learning to learn quickly for few-shot learning. *arXiv preprint arXiv:1707.09835*.
- Liu, S.; Johns, E.; and Davison, A. J. 2019. End-to-end multi-task learning with attention. In *Proceedings of the IEEE/CVF conference on computer vision and pattern recognition*, 1871–1880.
- Majee, A.; Agrawal, K.; and Subramanian, A. 2021. Few-shot learning for road object detection. In *AAAI Workshop on Meta-Learning and MetaDL Challenge*, 115–126. PMLR.
- Mnih, V.; Heess, N.; Graves, A.; et al. 2014. Recurrent models of visual attention. *Advances in neural information processing systems*, 27.
- Mnih, V.; Kavukcuoglu, K.; Silver, D.; Graves, A.; Antonoglou, I.; Wierstra, D.; and Riedmiller, M. 2013. Playing atari with deep reinforcement learning. *arXiv preprint arXiv:1312.5602*.
- Nikpour, B.; and Armanfard, N. 2021. Joint selection using deep reinforcement learning for skeleton-based activity recognition. In *2021 IEEE International Conference on Systems, Man, and Cybernetics (SMC)*, 1056–1061. IEEE.
- Nikpour, B.; and Armanfard, N. 2023a. Spatial Hard Attention Modeling via Deep Reinforcement Learning for Skeleton-Based Human Activity Recognition. *IEEE Transactions on Systems, Man, and Cybernetics: Systems*.
- Nikpour, B.; and Armanfard, N. 2023b. Spatio-temporal hard attention learning for skeleton-based activity recognition. *Pattern Recognition*, 139: 109428.
- Nikpour, B.; Sinodinos, D.; and Armanfard, N. 2022. Deep reinforcement learning in human activity recognition: A survey.
- Rangrej, S. B.; and Clark, J. J. 2021. A probabilistic hard attention model for sequentially observed scenes. *arXiv preprint arXiv:2111.07534*.
- Ranzato, M. 2014. On learning where to look. *arXiv preprint arXiv:1405.5488*.
- Ravi, S.; and Larochelle, H. 2016. Optimization as a model for few-shot learning. In *International conference on learning representations*.
- Ren, M.; Liao, R.; Fetaya, E.; and Zemel, R. 2019. Incremental few-shot learning with attention attractor networks. *Advances in neural information processing systems*, 32.
- Seifi, S.; Jha, A.; and Tuytelaars, T. 2021. Glimpse-attend-and-explore: Self-attention for active visual exploration. In *Proceedings of the IEEE/CVF International Conference on Computer Vision*, 16137–16146.
- Shi, G.; Chen, J.; Zhang, W.; Zhan, L.-M.; and Wu, X.-M. 2021. Overcoming catastrophic forgetting in incremental few-shot learning by finding flat minima. *Advances in neural information processing systems*, 34: 6747–6761.
- Snell, J.; Swersky, K.; and Zemel, R. 2017. Prototypical networks for few-shot learning. *Advances in neural information processing systems*, 30.
- Vella, D.; and Ebejer, J.-P. 2022. Few-shot learning for low-data drug discovery. *Journal of Chemical Information and Modeling*, 63(1): 27–42.
- Wang, X.; Chen, W.; Wu, J.; Wang, Y.-F.; and Wang, W. Y. 2018. Video captioning via hierarchical reinforcement learning. In *Proceedings of the IEEE conference on computer vision and pattern recognition*, 4213–4222.
- Wang, Y.-X.; Gui, L.; and Hebert, M. 2017. Few-shot hash learning for image retrieval. In *Proceedings of the IEEE International Conference on Computer Vision Workshops*, 1228–1237.
- Welinder, P.; Branson, S.; Mita, T.; Wah, C.; Schroff, F.; Belongie, S.; and Perona, P. 2010. Caltech-UCSD birds 200.
- Williams, R. J. 1992. Simple statistical gradient-following algorithms for connectionist reinforcement learning. *Machine learning*, 8(3-4): 229–256.



Yan, S.; Zhang, S.; He, X.; et al. 2019. A Dual Attention Network with Semantic Embedding for Few-Shot Learning. In *AAAI*, volume 33, 9079–9086.

Yun, S.; Choi, J.; Yoo, Y.; Yun, K.; and Young Choi, J. 2017. Action-decision networks for visual tracking with deep reinforcement learning. In *Proceedings of the IEEE conference on computer vision and pattern recognition*, 2711–2720.